Available online at www.sciencedirect.com
ScienceDirect
Catalysis Today 131 (2008) 61–69
CATALYSIS TODAY
www.elsevier.com/locate/cattod

Dendritic SBA-15 supported Wilkinson's catalyst for hydroformylation of styrene

P. Li, S. Kawi *

Department of Chemical & Biomolecular Engineering, National University of Singapore, 10 Kent Ridge Crescent, Singapore 119260, Republic of Singapore

Available online 21 December 2007

Abstract

After PAMAM (polyamidoamine) dendrimers have been successfully grown in SBA-15 mesoporous materials, Wilkinson's catalyst ($RhCl(PPh_3)_3$) precursor has been tethered on these dendritic supports to produce heterogeneous catalysts for hydroformylation reaction of styrene. SBA-15 has been functionalized by two methods. In the passivation method, the silanols outside the SBA-15 pores have been passivated to preclude the rhodium precursor to be tethered outside the channels. The rhodium catalysts supported in the pore channels of this passivated SBA-15 show positive dendritic effects in enhancing the catalytic activity, regio-selectivity and stability of the catalyst by minimizing the leaching of the rhodium complex catalyst from the catalyst support to the liquid-phase media.

Keywords: Wilkinson's catalyst; Passivation; SBA-15; Hydroformylation; Styrene

1. Introduction

As the largest industrial catalytic process, hydroformylation reaction has been the subject of intensive studies [1,2]. The linear aliphatic aldehydes derived from this reaction are important industrial chemical intermediates, which can be further oxidized to acids or reduced to alcohols. The branched aromatic aldehydes products from this reaction are crucial to the pharmaceutical industry as they have been used as intermediates in the synthesis of pharmaceutical compounds. For example, in the synthesis of anti-inflammatory agents, such as ibuprofen and naproxen, the branched aldehydes of 4-isobutylstyrene and 6-methoxy-2-vinylnaphthalene have been mildly oxidized, respectively to produce the products [3]. Therefore styrene has often been chosen as a model substrate for hydroformylation reaction [4,5]. However, such a versatile reaction faces with serious problems of separating the reaction products from the liquid phase for decades. Tremendous efforts have been directed to synthesize an ideal catalytic system, which combines the advantages from both homogeneous and heterogeneous catalysis [6,7]. Although solid supports such as [8–12] zeolite, silica, alumina and polymers, etc. have been tested as catalyst supports for producing heterogeneous catalysts, however these catalyst supports are usually accompanied with a significant loss in activity and selectivity.

In recent years, dendrimer [13,14], a novel material, has been synthesized and applied to catalysis since its highly branched structures can provide multiple sites for coordination with transition metal complexes. Although dendrimer is soluble in organic solvent, it can be separated from liquid phase through nano-filtration. Moreover, the coordination of dendrimer with transition metal complexes may bring forth enhanced catalytic performance due to positive dendritic effect [15,16]. Bourque et al. reported the immobilization of rhodium on PAMAM dendrimer supported on silica gel, producing a highly active and regio-selective catalyst for hydroformylation of aryl olefins and vinyl esters [17]. Recently, MCM-41 has been employed as a highly order mesoporous catalyst support to grow dendrimer [18,19]. The combination of the highly ordered mesoporous material with the nanosized highly branched dendrimer creates a distinct architecture which is helpful for the dispersion of rhodium species due to the high surface area of support and the multiple binding sites of dendrimer for the enhancement of regio-selectivity perhaps due to the dendrimer effect and the pore effect [20]. However, the first generation G(1) and second generation G(2) catalysts did not have high loading of rhodium

* Corresponding author.
E-mail address: chekawis@nus.edu.sg (S. Kawi).

0920-5861/$ – see front matter © 2007 Published by Elsevier B.V.
doi:10.1016/j.cattod.2007.10.090

species although higher generation dendrimers are supposed to have more loading due to more binding dendritic sites. The result suggests that during the growth of dendrimers in mesoporous material, the shrinking pore volume and surface area impaired the binding sites. The result also suggests that some portion of dendrimer have been grown outside the external surfaces of the MCM-41 pores due to the greater accessibility of external surfaces to grow dendrimers [21]. To prevent the leaching of transition metal complexes, Thomas et al. [22] and Mukhopadhyay et al. [23,24] functionalized the internal pores of MCM-41 by passivating the silanols outside the MCM-41 channels so that the surface ligands could be functionalized only within the pores and the transition metal complexes could be tightly bound inside the pores. A comparison between the catalysts with and without external passivation shows that the latter has high leaching of transition metal complexes while the former is quite stable as it has no leaching [24].

In this study, SBA-15 [25] has been employed as mesoporous support for growing PAMAM dendrimers in order to immobilize the Wilkinson's catalyst for the hydroformylation of styrene. The dendritic catalysts based on functionalized SBA-15 with passivation of silanols outside the SBA-15 mesopore channels exhibit superior catalytic performance than the non-passivated SBA-15 supported catalysts.

2. Experimental

2.1. Chemicals

3-Aminopropyltriethoxysilane (APES), tetraethylorthosilicate (TEOS), methyl acrylate (MA), ethylene diamine (EDA), dichlorodiphenylsilane (Ph_2SiCl_2), P123 and Wilkinson's catalyst ($RhCl(PPh_3)_3$) were all commercially purchased. Reactions involving air-sensitive compounds were performed using a Schlenk line under a positive pressure of purified nitrogen. All the solvents were refluxed with freshly cut sodium chips and benzophenone until the color was intense blue.

2.2. Synthesis of pure SBA-15

SBA-15 was prepared following the synthesis procedures reported in literatures [25,26]. Pluronic P123 triblock copolymer was used as surfactant template. The molar composition of gel was 1 SiO_2:0.017 P123:2.9 HCl:202.6 H_2O. The surfactant Pluronic P123 was dissolved in the mixture of water and HCl at 40 °C. After the solution was clear, TEOS was added to the surfactant solution and the mixture was then transferred to a polypropylene bottle and heated at 100 °C for 2 days. The white solid was filtered and washed with deionized water until no bubble could be found in the filtrate. Then the filtered pure white powder was transferred to a crucible to be dried at 50 °C in oven overnight. To remove the organic template from the mesopores, the as-synthesized SBA-15 was calcined at 550 °C (with the ramping rate of 5 °C/min) for 8 h. The as-synthesized siliceous SBA-15 has a pore size distribution of 75 Å, pore volume of 1.36 cm^3/g and surface area of 750 m^2/g.

2.3. Pre-treatment of SBA-15

It has been reported [27] that there exists a weak physical interaction between MCM-41 surface and water molecules. The physisorbed water molecules interact with the surface either by Van Der Waals forces or by hydrogen bonds. Because the rhodium complexes to be tethered on the MCM-41 support are water sensitive, the physically adsorbed water molecules have to be removed from the surface of the support. According to literature [28], heating the MCM-41 material under vacuum at 200 °C for 6 h can remove the physically adsorbed water. Therefore, in this study, the SBA-15 support was pretreated under vacuum at 200 °C for 12 h in order to remove the physically adsorbed water molecules prior to functionalization.

2.4. Synthesis of dendritic supports

In this study, two methods were used to functionalize the internal pore surfaces of SBA-15. The first method was via direct reaction of the surface silanols with APES to give aminated SBA-15 (NH_2). These amine groups are ''initiator sites'' which form zeroth generation of dendrimer on which higher generation of dendrimers would be grown. The second method was to passivate the silanols outside the mesopores of SBA-15 prior to functionalization, with the rest of the steps of functionalization and growing of dendrimers to be the same as those used in the first method.

2.4.1. Functionalization of non-passivated SBA-15

Preparation of dendrimer began with the introduction of amino groups, which act as ''initiator sites'' onto the mesoporous silica surface. This was achieved by the treatment of surface silanol groups with APES. Five grams of dried SBA-15 support and 150 ml of toluene solution containing 7.5 ml of APES (5.0%) were charged into a 250 ml three-neck flask, and the mixture was refluxed for 48 h under stirring with a magnetic stirrer. The functionalization of silanol groups is illustrated in Scheme 1. This functionalized SBA-15 with a monolayer of surface amine ligands both inside and outside the SBA-15 channels is named as ''S0'' in this study, as ''S'' stands for SBA-15 and ''0'' for zeroth generation of dendrimer.

2.4.2. Passivation of silanols before functionalization

Two grams of dried SBA-15 was slurried in 60 ml of THF (tetrahydrofuran) followed by 0.06 ml of Ph_2SiCl_2 was added to the slurry and the suspension was stirred for 1 h [21–23]. The reaction mixture was cooled to 195 K, and 1.0 ml of APES was added to the reaction mixture. The slurry was stirred for 3 h at 195 K, slowly warmed to ambient temperature, and then left at 50 °C for a further 20 h. The reaction mixture was then filtered, washed with copious amounts of THF (100 ml) and dried under

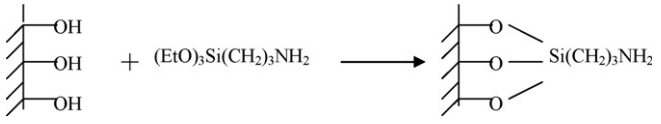

Scheme 1. Functionalization of SBA-15 by APES.

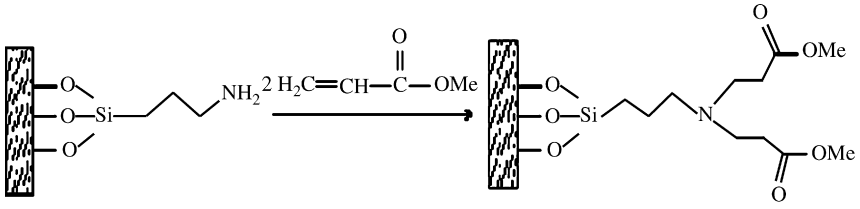

Scheme 2. Michael addition of methyl acrylate to amino groups on the surface of SBA-15.

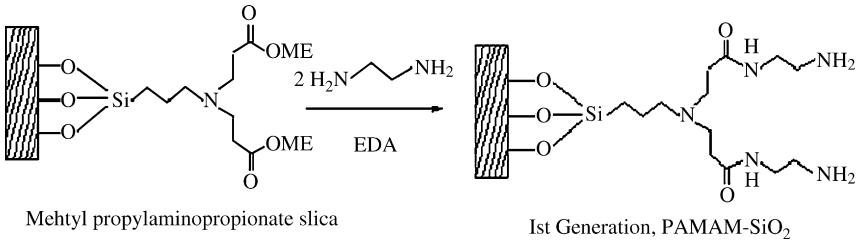

Scheme 3. Amidation of terminal groups on the surface of SBA-15 with EDA.

high vacuum. This passivated and functionalized SBA-15 with a monolayer of surface amine ligands inside the SBA-15 channels is named as "PS0" in this study, as "P" stands for passivation, "S" for SBA-15 and "0" for zeroth generation of dendrimer.

2.4.3. Grafting dendrimers on aminated SBA-15

Grafting reaction and propagation of PAMAM dendrimer from the silica surface were achieved by two alternate steps [29] as illustrated in Schemes 2 and 3.

Michael addition, which is the first reaction step in grafting dendrimer on SBA-15, was carried out as follows: 150 ml of ethanol and 2.5 ml of MA were added into a 250 ml three-neck flask containing functionalized SBA-15 (PS0 or S0). The mixture was refluxed for 24 h under stirring with a magnetic stirrer. After the Michael reaction, the resulting silica was filtered and washed by anhydrous ethanol.

Amidation of terminal ester groups, which is the second step, was carried out as follows: 150 ml of ethanol and 10 ml of EDA were added into the 250 ml three-neck flask containing the silica. The mixture was stirred with a magnetic stirrer and refluxed for 24 h. The resulting silica was washed with anhydrous ethanol (4× 30 ml). Alternate Michael addition and amidation steps were conducted repeatedly to propagate the dendrimer to 2nd and 3rd generations. These SBA-15 supported dendrimers are named as PSn (n = 0, 1, 2, 3) or Sn (n = 0, 1, 2, 3) based on whether SBA-15 has been passivated or not. "P" stands for passivation, "S" for SBA-15 and "n" for the generation number of the supported dendrimer. Theoretically, in Gn dendrimer (i.e. the nth generation of dendrimer), there are 2^n of branches of the amide (–CONH–) group linked with the terminal amine group (–NH_2).

2.4.4. Tethering of Rh precursor to dendritic SBA-15 support

In this study, dendritic SBA-15 supports were reacted with $RhCl(PPh_3)_3$ by coordination of the surface ligand donors to the rhodium precursor to produce SBA-15 tethered rhodium catalysts, which are designated as WSn ((n = 0, 1, 2, 3) or WPSn (n = 0, 1, 2, 3), where W stands for the Wilkinson's catalyst precursor. The whole procedure for the preparation of tethered rhodium complex catalysts was carried out under nitrogen (99.999% purity) atmosphere so that there would be no exposure of the catalyst to air or moisture as such exposure may affect the catalytic activity of the supported rhodium catalyst. The catalysts were designed to contain 2 wt.% of rhodium (i.e. 0.194 mmol Rh/g of catalyst support).

After dissolving 90 mg of $RhCl(PPh_3)_3$ in 60 ml toluene, 0.5 g of PS0 or S0 was added to the solution and the mixture was stirred and refluxed overnight at 110 °C (Scheme 4.). After cooling down to room temperature, the mixture was filtered and the separated solid was washed with toluene (4× 20 ml) and then dried under vacuum at room temperature. The freshly synthesized yellow-brown catalyst was stored under nitrogen atmosphere. The tethering of Rh precursor was the same for those involving higher generation dendritic SBA-15 supports. It should be noted that all PSn (n = 0, 1, 2, 3) and Sn (n = 0, 1, 2, 3) samples were dehydrated at 120 °C under vacuum for 12 h before they were used to tether Wilkinson's catalyst.

2.5. Hydroformylation of styrene

The hydroformylation reactions were carried out at 20 bar of CO/H_2 (1:1) gas mixture at temperature of 80 °C. The substrate chosen was styrene and the solvent was THF. The required amount of the styrene and the solvent, for one reaction, was 3 and 50 ml, respectively. For each experiment, 0.15 g of

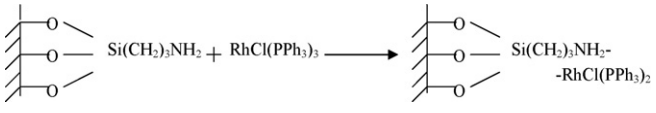

Scheme 4. Tethering of $RhCl(PPh_3)_3$ on SBA-15(NH_2).

heterogenized catalyst was transferred into the Parr reactor under nitrogen atmosphere and the THF was pumped into the reactor. After the reaction system reached the temperature required for the reaction, styrene was then pumped into the reactor. The whole reaction system was flushed with syn-gas before the reaction.

2.6. Instrument

X-ray diffraction (XRD) analysis was carried out using a Shimadzu XRD-6000 X-ray powder diffractometer (Shimadzu, Japan), where Cu target Kα-ray (operating at 40 kV and 30 mA) was used as the X-ray source. The scanning range (2θ) was from 1.5° to 10.0° with a scanning speed of 2.0°/min using a continuous scan mode. The sample was finely grounded and placed into an aluminum sample holder having an 18 mm × 18 mm × 2 mm opening.

The infrared spectra characterizing the passivated SBA-15 supported dendrimers from zeroth to 3rd generation were measured with Shimadzu FTIR-8700 spectrometer (Shimadzu, Japan) under a resolution of 2 cm^{-1}. To obtain good FTIR spectra, 15 mg of sample was pressed into self-supported wafer.

Gas chromatograph-flame ionization detection (GC-FID) on the Perkin-Elmer Auto System XL was used to identify the reactants and products during or after reactions. The non-polar capillary column used was HP-5MS (cross-linked 5% phenyl methyl siloxane) with a length of 30 m and a diameter of 0.25 mm.

The thermogravimetric (TGA) and differential thermal (DTA) analyses of PSn ($n = 0$, 1, 2, 3) were performed simultaneously on a SHIMADZU DTG-50 thermogravimetric analyzer. The sample was heated in air with a flow rate of 50 ml/min under a heating rate of 10 °C/min.

The weight content of the rhodium metal in the catalysts was determined by inductively coupled plasma atomic emission (ICP). For ICP measurements, 0.05 g of solid sample was first dissolved in 5 ml of hydrofluoric acid (HF, 40%) at 100 °C in a Teflon bottle to dissolve the silica component of the sample. After hydrofluoric acid was evaporated, 1 ml of nitric acid (65%) and 5 ml of 5 M hydrochloric acid were added into the reaction mixture to completely dissolve the left rhodium metal. 20 ml of deionized water was added into the mixture and heated at 100 °C for 1 h to evaporate nitric acid and hydrochloric acid. After that the solution was cooled down to room temperature and then diluted by deionized water in a 25 ml volumetric flask.

3. Results and discussions

3.1. Characterization

3.1.1. FTIR analysis

Fig. 1 shows the FTIR spectra characterizing the growth of PAMAM dendrimers from zeroth to 3rd generation inside the passivated SBA-15 support, with each spectrum showing the growth of half generation of dendrimer. The peak around 1640 cm^{-1} of G0 is attributed to the amino groups, indicating that after functionalization the surface amine ligands $-NH_2$ were successfully grown on the mesoporous siliceous SBA-15. After Michael addition reaction, the amino group peak disappears while another peak around 1715 cm^{-1} appears. The peak around 1715 cm^{-1}, which is clearly visible in all half-generations, is attributed to the ester bond of the half generation of dendrimer (designated as Gn.5, where $n = 0$, 1, 2). After the amidation reaction, which immediately follows the Michael addition reaction, the ester bond peak disappears whereas the peak around 1655 cm^{-1}, which is assigned to amide band I and the peak around 1550 cm^{-1}, which is assigned to amide band II, appear. Since these two peaks are clearly visible in all integer-generations from 1st to 3rd, the appearance of these two peaks shows that the first generation of dendrimer has been successfully grown on the SBA-15 mesoporous support. Through the iteration of the Michael addition followed by amidation reaction steps, the dendrimer grows to higher generations, where the arms of the dendrimer are amplified and the terminal functional groups are increased exponentially. The peaks in the FTIR spectra not only show the appearance and disappearance of the functional groups but also demonstrate the increase of the intensity of the peaks from 1st to 3rd generation, showing the amplification of the generation of dendrimers. Although these FTIR results are similar to literature report [18], it is difficult to use the FTIR spectroscopy to carry out the quantitative analysis to show how much dendrimer in mass has grown from one generation to the next. TGA results will be discussed in the next section to help answer this question.

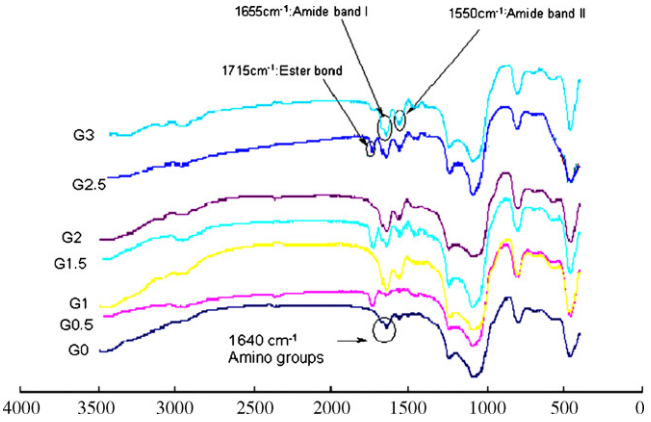

Fig. 1. FTIR spectra characterizing the passivated SBA-15 supported dendrimers from zeroth to 3rd generation.

3.1.2. TGA analysis

Fig. 2a–d shows the TGA and DTA analysis curves for the passivated SBA-15 supported PSn ($n = 0$, 1, 2, 3) dendrimers. It is clear that for all the samples the weight loss accompanied with absorption of heat below around 100 °C is associated with water desorption. The weight loss line between 100 and 800 °C was used as a baseline amount for the passivated SBA-15-based dendritic samples to correct for the weight loss in these samples. The large DTA peak between 250 and 390 °C is assigned to the pyrolysis of the carbon–silica bond. The second large shoulder peak at around 550 °C is assigned to the deep combustion of carbonaceous species (coke), which was formed

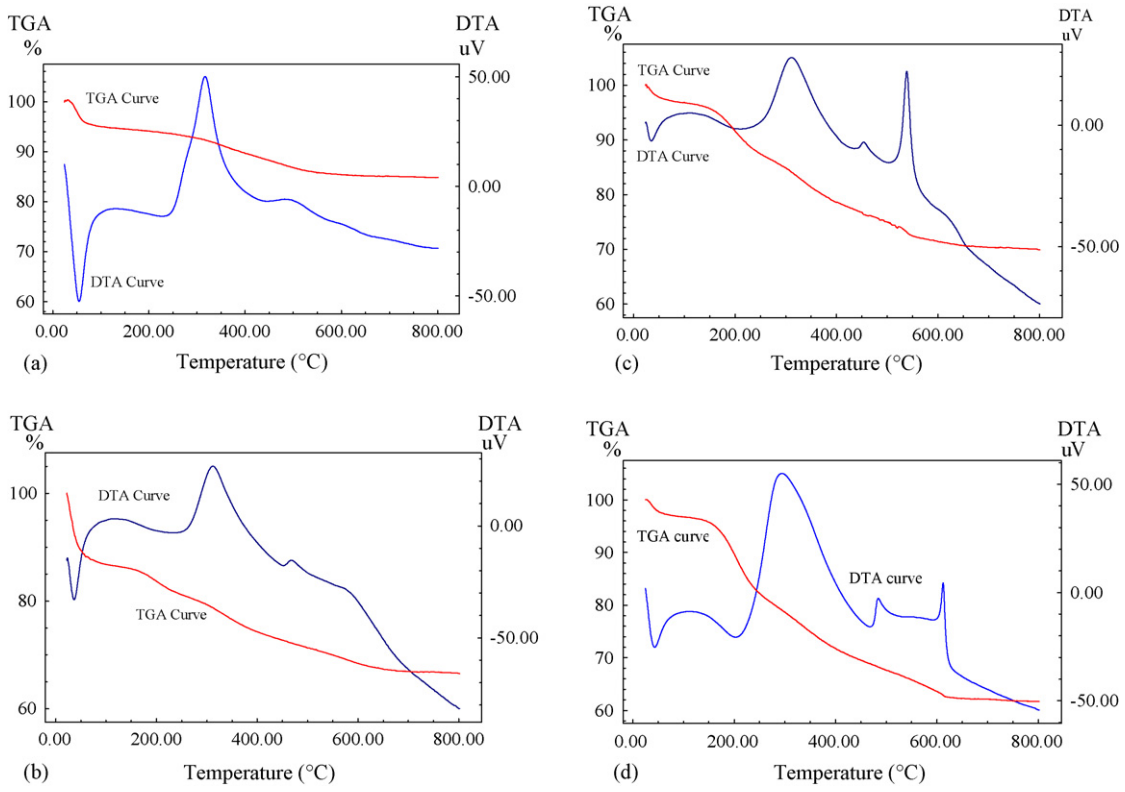

Fig. 2. (a) TGA and DTA analysis of PS0, (b) TGA and DTA analysis of PS1, (c) TGA and DTA analysis of PS2 and (d) TGA and DTA analysis of PS3.

during the pyrolysis of the aminopropyl groups at around 300 °C [18]. This shoulder peak at around 550 °C is consistently observed in all the PSn ($n = 1, 2, 3$) samples, indicating that the functional groups are similar in architecture for different generations of dendrimer. Since no endothermic peak can be attributed to component other than water, this result also shows that the synthesis reaction for growing dendrimer on SBA-15 mesoporous support is perfect from the half-generation to integer-generation; otherwise, the endothermic peak for the decomposition of ester species would appear at some temperature lower than that of the fully grown dendrimer.

3.1.3. XRD analysis

Fig. 3 shows the small angle XRD patterns of synthesized SBA-15, PS3 and used WPS3 catalyst (which is designated as UWPS3). SBA-15 and PS3 display three resolved peaks corresponding to diffraction planes of (1 0 0), (1 1 0) and (2 0 0), indicating that these synthesized materials possess the highly ordered mesoporous hexagonal structures [25]. Although used WPS3 catalyst (UWPS3) shows a strong peak at a theta angle of around 0.8–1.0° which is dwarfed by the other two peaks, the characteristic XRD pattern of the used catalyst still remains similar to that of SBA-15 as reported in literature. The diffraction peaks of PS3 become only slightly lower and broader than that of the pure SBA-15, showing that the synthesis steps used in passivating silanols, in growing generations of dendrimers even up to third generation as well as in tethering the rhodium precursor to the dendritic support have very little damaging effects to the mesoporous structure of SBA-15. Although the diffraction peaks of used WPS3 are much lower and broader than that of the pure SBA-15, the diffraction patterns of used WPS3 catalyst maintain the SBA-15 characteristic structures, demonstrating the robust stability of the dendritic SBA-15 supported Wilkinson's catalyst during the high-pressure liquid phase hydroformylation process.

3.1.4. TEM analysis

Fig. 4a and b shows the TEM images of used WPS3 catalyst, with the former taken perpendicularly to the SBA-15 channels and the latter taken parallel to the SBA-15 channels. The results show that, after hydroformylation of styrene, the catalyst structure still maintains the hexagonal array of 1D mesopore channels and 2D p6 mm hexagonal of SBA-15 as reported by

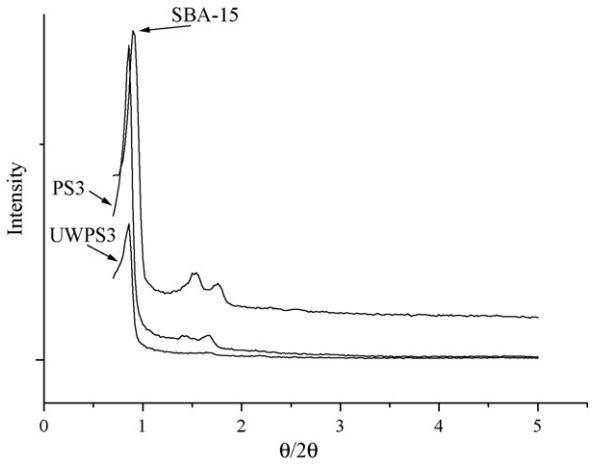

Fig. 3. XRD patterns of pure SBA-15, PS3 and used WPS3 catalyst (UWPS3).

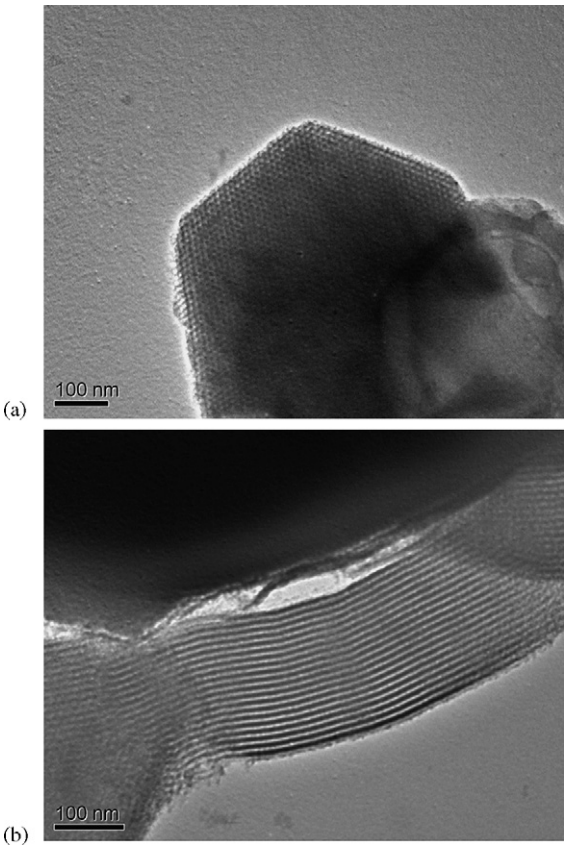

Fig. 4. (a) Cross-section TEM image of used WPS3 catalyst and (b) vertical section TEM image of used WPS3 catalyst.

Zhao et al. [25]. The TEM results also corroborate the XRD results that the catalyst is stable during the hydroformylation process. No metallic rhodium particles are observed on the surface, indicating that the rhodium species were dispersed very well inside the pore channels of SBA-15. The TEM results suggest that the passivation of external silanol groups helps the rhodium species to be tethered and dispersed inside the SBA-15 mesopores.

3.1.5. ICP analysis

Table 1 shows the ICP analysis of the rhodium content in the fresh and used WSn as well as WPSn catalysts. From WS0 to WS3 the weight percentage loss of rhodium after hydroformylation reaction is 0.63, 0.37, 0.24 and 0.19 wt.%, respectively. For WPS0 to WPS3 catalysts, the percentage loss of rhodium is 0.15, 0.12, 0.11 and 0.13 wt.%, respectively. It is obvious that the non-passivated SBA-15 supported catalysts (WSn catalysts) exhibit much higher leaching problem than the passivated SBA-15 supported catalysts (WPSn catalysts). This result shows that the tethering of Wilkinson's catalyst could be either outside or inside the SBA-15 pore channels. In the non-passivated SBA-15 supported catalysts, a substantial amount of homogeneous rhodium precursor is anchored outside the SBA-15 pore channels where a substantial amount of external surface ligands are readily available and more easily accessible to rhodium precursor than the ones inside the pore channels. The rhodium species that is tethered outside the SBA-15 pore channels tends to leach more than the one inside the pore channels. Therefore the non-passivated SBA-15 supported catalyst has a serious leaching of rhodium species from the support to the liquid phase medium during hydroformylation reaction. This is in agreement with the literature result [23].

Table 1
ICP Analysis of rhodium content in non-passivated and passivated SBA-15 supported rhodium catalysts with different generation of dendrimer

Catalyst	Rh% (before reaction)	Rh% (after reaction)
WS0	1.87	1.24
WS1	1.64	1.27
WS2	1.52	1.28
WS3	1.01	0.82
WPS0	1.24	1.09
WPS1	1.55	1.43
WPS2	1.51	1.40
WPS3	1.09	0.96

It should also be noted that for the WSn catalysts, the rhodium loading decreases as the PAMAM generation increases, whereas for the WPSn catalysts, WPS1 and WPS2 are the two passivated catalysts that contain the highest rhodium loading. This may be explained by the fact that, although the S0 has a lot of amine groups outside the SBA-15 channels, but as the PAMAM generation is grown from these amine groups, the growth of dendrimer is not perfect and a lot of defects occur in the dendrimer branches [17]. However, for the WPS0, as most external silanols have been passivated before functionalization, only the internal amine groups participate in the tethering of rhodium precursors, resulting in less rhodium loading. However, the growth of PAMAM dendrimer from PS0 to PS1 is more perfect than that from S0 to S1 due to the larger surface areas inside the SBA-15 channels, which lead to less crowdedness. Therefore WPS1 and WPS2 possess more rhodium loading than WPS0. However, for WPS3, the space inside the SBA-15 pore channels is so congested that it fails to bind more rhodium precursors than those containing lower generation of dendrimer. Nevertheless, the ICP analysis indicates that the higher generation of PAMAM dendrimer is helpful in minimizing the leaching of rhodium species during the hydroformylation reaction due to the longer dendrimer arms binding the rhodium species more efficiently.

3.2. Catalysis run

3.2.1. Activity

In Fig. 5, the non-passivated SBA-15-based dendritic catalysts WS0, WS1, WS2 and WS3 demonstrate a descending order of activity from zeroth generation to third generation of dendrimer. Although this order is in good agreement with literature results on MCM-41-based dendritic catalysts [18], the difference between these two mesoporous supports is that the dendrimer generation for SBA-15 has been increased to the third generation, whereas MCM-41, which has smaller pores than SBA-15, could only accommodate second generation of dendrimers in the pores [19,30–32]. The decrease of catalytic

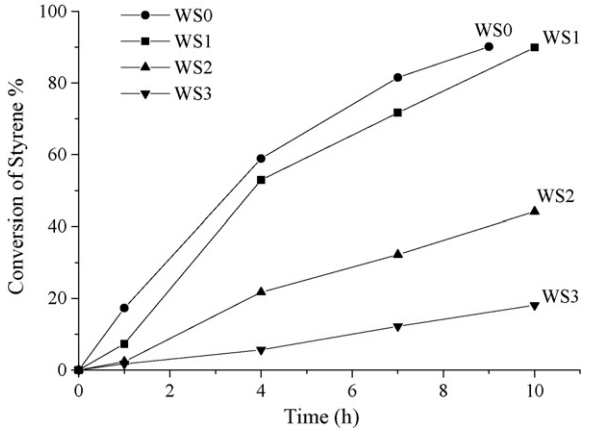

Fig. 5. Catalytic activity of WSn catalysts ($n = 0, 1, 2, 3$) for styrene hydroformylation.

activity from one generation to the next can be explained by the shrinking of pore size as higher generation of dendrimers grown inside the pores could increase the diffusion resistance to the reactants, which is a characteristic problem of heterogeneous catalysis [33].

The activity results associated with the passivated SBA-15-based catalysts shed light on some other delicate underling factors influencing the activity of the catalysts. Fig. 6 shows the order of catalytic activity of the passivated WPSn catalysts as follows: WPS0 > WPS2 > WPS3 > WPS1; this catalytic activity order of passivated catalysts is different from that of the non-passivated SBA-15-based WSn catalysts, with the exception that both catalysts have the highest activity for the zeroth generation of dendrimer. This is because either WS0 or WPS0 catalyst has the largest pore size among the non-passivated and passivated catalysts, respectively. Therefore, the catalyst containing the zeroth generation of dendrimer has the least diffusion resistance to the reactants.

The ICP results indicate that the highest catalytic activity shown by WS0 is also likely attributed to the highest percentage amount of rhodium leaching into the liquid phase. From WPS0 to WPS1, the catalytic activity drops due to the increase of diffusion resistance. The drop in activity for the passivated catalyst from WPS0 to WPS1 is more appreciable than the difference of activity between WS0 and WS1, possibly because WS0 and WS1 have so high amount of leaching of rhodium species into the liquid phase, making the catalysis on WS0 and WS1 similar to a mixed homogeneous and heterogeneous catalysis.

Furthermore, from WS0 to WS1, the partial ramification of dendrimer growing outside the pores and the congestion of the inner pore of SBA-15 are not as palpable as that of the passivated SBA-15 where the dendrimer grows utterly inside the pores. On the other hand, the leached rhodium species can blur the difference of activity due to the supports.

The increase of activity from WPS1 to WPS2 is in contrast to the decrease of activity from WS1 to WS2. Although the pore size keeps on shrinking from WPS1 to WPS2, and hence there is an increasing diffusion resistance from WPS1 to WPS2, however there is a promotional dendrimer effect [15,16,34,35] due to the increasing amount of binding sites attributed to the dendrimer growth.

Since the synergistic cooperation of the catalytic centers inside the pores counterbalances the negative effect attributed to the decrease of pore size, the promotional dendrimer effect makes WPS2 the more active catalyst than WPS1. It should be noted that WPS2 has a similar loading amount of rhodium but less leaching as compared to WPS1. Meanwhile, from WS1 to WS2, as the dendrimers grow both inside and outside the pores, the entanglement of dendrimer arms outside the pores begins to be a dominant hindrance for the catalytic activity. Similarly, this holds true for WS2 and WS3. From WPS2 to WPS3, the diffusion resistance becomes so severe that even the positive dendritic effect cannot compensate its retarding effect to the catalyst; therefore the activity decreases from WPS2 to WPS3.

3.2.2. Regio-selectivity

Fig. 7 shows the regio-selectivity of WS0, WS1, WS2 and WS3 catalysts along with time. Among these catalysts, WS0 exhibits the highest regio-selectivity, with the order of regio-selectivity as follows: WS0 > WS1 ≧ WS2 > WS3. The regio-selectivity order of WS0, WS1, WS2 and WS3 catalysts is similar to their activity order. The highest regio-selectivity

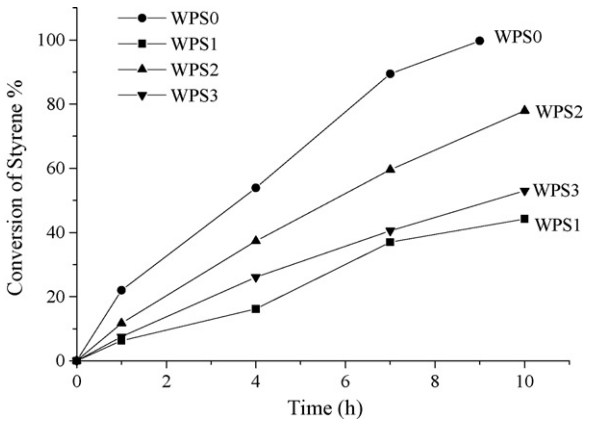

Fig. 6. Catalytic activity of WPSn catalysts ($n = 0, 1, 2, 3$) for styrene hydroformylation.

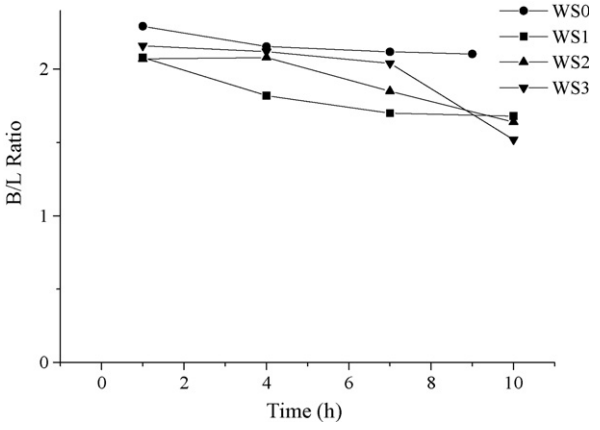

Fig. 7. Catalytic regio-selectivity of WSn catalysts ($n = 0, 1, 2, 3$) for styrene hydroformylation (B/L is the ratio between 2-phenylpropionaldehyde and 3-phenylpropionaldehyde product).

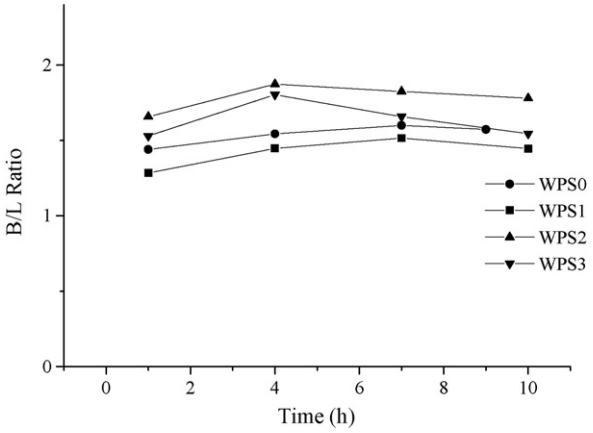

Fig. 8. Catalytic regio-selectivity of WPSn catalysts (n = 0, 1, 2, 3) for styrene hydroformylation.

shown by WS0 is mainly due to leaching of rhodium. Based on the mechanism of homogeneous hydroformylation, both the electronic and steric effects of the catalytic center are the governing factors controlling the final regio-selectivity of the reaction as well as branch to linear aldehyde ratio [36].

By nature, styrene favors initial Markownikov addition to Rh–H, with subsequent steps leading to more branch aldehyde product due to the electronic factors within styrene. This is because the phenyl in styrene is a strong electron-withdrawing group which induces the C=C to be slightly polarized, resulting in the terminal carbon to possess slightly positive charge and the internal carbon slightly negative charge ($C^{\sigma-} = C^{\sigma+}$). Accordingly, the polarity of Rh–H influences the distribution of the final products as it directs the initial addition of the double bond of the alkene. A stronger π acid in the coordination sphere of the Rh makes H less hydridic and less Markownikov addition for styrene [37]. Therefore, when PPh_3 is replaced by $–NH_2$, the catalyst favors more branch aldehyde products due to the electronic effect, whereas PPh_3 promotes more branch aldehyde products due to the steric effect because the branch intermediates have less steric hindrance than the linear counterpart in the presence of the phenyl group.

From WS0 to WS3, WSn (n = 1, 2, 3) does not gain much advantage from the electronic effect to produce more branch aldehyde product since all the surface amine ligands are similar regardless of the generation of dendrimer. Nevertheless, the crowdedness of the entanglement of dendrimer arms which rampantly grow outside the SBA-15 channels simply makes the catalytic center lose specificity, suggesting that the higher the generation of dendrimer is, the less the regio-selectivity [38].

Since one of the main objectives of this study is to explore and take advantage of the highly ordered mesoporous structures of SBA-15, such growth of the PAMAM dendrimers outside the pores obscures the pore effect and proves to be hindering both the catalytic activity and regio-selectivity. However, with the passivation of silanols outside the SBA-15 pores, the regio-selectivity results of WPSn catalysts (Fig. 8) complement and shed light on how the combination of dendrimer and the uniform mesoporous pore influences the regio-selectivity of the hydroformylation of styrene. In contrast with the regio-selectivity observed for WSn catalysts, the regio-selectivity of WPSn catalysts shows a different order from zeroth to third generation of dendrimer: WPS1 < WPS0 < WPS3 < WPS2. Along with the growth of dendrimer from zeroth to third generation, the regio-selectivity reaches a climax at the second generation of dendrimer, WPS2 and then decreases at higher generation. This is because from WPS0 to WPS1, the surface area of catalysts decreases, hence the heterogeneity of the catalyst accordingly increases and brings to a reduced regio-selectivity. However, from WPS1 to WPS2, the growth of dendrimer from the first to second generation inside the SBA-15 mesopores produces an ideal environment for the regio-selectivity of styrene hydroformylation due to the combination of positive dendrimer effect and the pore size of SBA-15 at the second generation of dendrimer. This synergistic effect from the combination of positive dendrimer effect and pore size of SBA-15 balances the negative effect from the decrease of surface area, making WPS2 to be the most selective catalyst among WPSn catalysts.

The reaction result also confirms that both the pore size of mesoporous material and the generation of dendrimer affect the regio-selectivity of the hydroformylation catalyst, and in certain case the combination of the two makes an optimal circumstance for regio-selectivity. This promotion of regio-selectivity is mainly from the steric advantage inherent in WPS2. Although WPSn and WSn are similar in electronic structure as both use surface amine ligands to anchor Rh species, the actual conformation of each surface ligand is not identical in these two types of catalysts as the crowdedness of each surface ligand is different and the space effect influences the conformation. However, in the non-passivated SBA-15 supports where dendrimers grow outside the pores, such synergistic effect from the pore and the generation of dendrimer is severely eclipsed and cannot be observed. Therefore, as dendrimer grows from WS0 to WS3, no promotional effect from dendrimer occurs to balance the negative effect from the shrinkage of surface areas. Although WPSn catalysts seem to be slightly less selective than WSn catalysts, WPSn catalysts leach much less percentage of rhodium species during the hydroformylation reaction than WPSn catalysts, making WPSn catalyst to be a stable supported rhodium catalyst for hydroformylation of styrene.

4. Conclusions

A novel technique for passivating the silanol groups outside the SBA-15 pore channels has been successfully employed to grow dendrimers inside the pore channels and to tether rhodium species specifically inside the dendritic SBA-15 channels. FTIR and TGA results confirm the growth of dendrimers. XRD and TEM results show the stability of the mesoporous structure of the dendritic SBA-15-based catalysts. TEM results also confirm that the rhodium species anchored inside the channels of the passivated SBA-15-based WPSn catalysts are highly dispersed. The catalytic results demonstrate the differences of catalytic behavior between WPSn and WSn catalysts in terms of activity and regio-selectivity. The ICP results show that the passivation

of silanols outside the SBA-15 pore channels leads to catalysts, which have much less leaching of rhodium species than the non-passivated counterparts.

In WPSn catalysts, a combination of the pore size and dendrimer generation shows a synergistic effect by influencing both the activity and selectivity of the catalysts for styrene hydroformylation. Therefore among the WPSn catalysts, there is a certain generation, which is optimal for activity or regio-selectivity. WPS2 shows the best catalytic performance for regio-selectivity, which is the outcome of the interplay between pore size and generation of dendrimer.

Reference

[1] F. Ungvary, Coordin. Chem. Rev. 170 (1998) 245.
[2] M. Lenarda, L. Storaro, R. Ganzerla, J. Mol. Catal. A: Chem. 111 (1996) 203.
[3] B.G. Reuben, H.A. Wittcoff, Pharmaceutical Chemicals in Perspective, John Wiley, New York, 1989.
[4] J.A.J. Breuzard, M.L. Tommasino, F. Touchard, M. Lemaire, M.C. Bonnet, J. Mol. Catal. A: Chem. 156 (2000) 223.
[5] D.R. Inmaculada, O. Pamies, P.W.N.M. van Leeuwen, C. Claver, J. Organomet. Chem. 608 (2000) 115.
[6] J.H. Chen, H. Alper, J. Am. Chem. Soc. 119 (1997) 893.
[7] A.N. Ajjou, H. Alper, J. Am. Chem. Soc. 120 (1998) 1466.
[8] L. Huang, S. Kawi, Catal. Lett. 90 (2003) 165.
[9] W.A. Weber, B.L. Phillips, B.C. Gates, Chem. A: Eur. 5 (1999) 2899.
[10] K. Nozaki, Y. Itoi, F. Shibahara, E. Shirakawa, T. Ohta, H. Takaya, T. Hiyama, J. Am. Chem. Soc. 120 (1998) 4051.
[11] S. Alini, A. Bottino, G. Capannelli, A. Comite, S. Pananelli, Appl. Catal. A: Gen. 292 (2005) 105.
[12] S.M. Lu, H. Alper, J. Am. Chem. Soc. 125 (2003) 13126.
[13] D.A. Tomalia, J.R. Dewald, M.J. Hll, S.J. Martin, P.B. Smith, Preprints of the 1st SPSJ International Polymer Conference, Soc. Polym. Sci., Japan, Kyoto, (1984), p. 65.
[14] D.A. Tomalia, V. Berry, M. Hall, D.M. Hedstrand, Macromolecules 20 (1987) 1164.
[15] M.T. Reetz, G. Lohmer, R. Schwickardi, Angew. Chem. Int. Ed. Engl. 36 (1997) 1526.
[16] R. Breinbauer, E.N. Jacobsen, Angew. Chem. Int. Ed. Engl. 39 (2000) 3604.
[17] S.C. Bourque, F. Maltais, W.J. Xiao, O. Tardif, H. Alper, P. Arya, L.E. Manzer, J. Am. Chem. Soc. 121 (1999) 3035.
[18] J.P.K. Reynhardt, Y. Yang, A. Sayari, H. Alper, Chem. Mater. 16 (2004) 4095.
[19] J.P.K. Reynhardt, Y. Yang, A. Sayari, H. Alper, Adv. Funct. Mater. 15 (2005) 1641.
[20] C.T. Kresge, M.E. Leonowicz, W.J. Roth, J.C. Vartuli, J.S. Beck, Nature 359 (1992) 710.
[21] D.S. Shephard, W.Z. Zhou, T. Maschmeyer, J.M. Matters, C.L. Roper, S. Parsons, B.F.G. Johnson, M.J. Duer, Angew. Chem. Int. Ed. Engl. 37 (1998) 2719.
[22] T. Maschmeyer, R.D. Oldroyd, G. Sankar, J.M. Thomas, I.J. Shannon, J.A. Klepetko, A.F. Masters, J.K. Beattie, C.R.A. Catlow, Angew. Chem. Int. Ed. Engl. 36 (1997) 1639.
[23] K. Mukhopadhyay, A.B. Mandale, R.V. Chaudhari, Chem. Mater. 15 (2003) 1766.
[24] K. Mukhopadhyay, B.R. Sarkar, R.V. Chaudhari, J. Am. Chem. Soc. 124 (2002) 9692.
[25] D.Y. Zhao, Q. Huo, J.L. Feng, B.F. Chmelka, G.D. Stucky, J. Am. Chem. Soc. 120 (1998) 6024.
[26] H.H.P. Yiu, P.A. Wright, N.P. Botting, J. Mol. Catal. B: Enzyme 15 (2001) 81.
[27] S. Inagaki, Y. Fukushima, K. Kuroda, K. Kuroda, J. Colloid Interf. Sci. 180 (1996) 623.
[28] D. Brunel, A. Cauvel, F. Fajula, F. DiRenzo, MCM-41 type silicas as supports for immobilized catalysts, in: L. Bonneviot, S Kaliaguine (Eds.), Zeolites: A Refined Tool for Designing Catalytic Sites, Elsevier, 1995 p. 173.
[29] J. Bu, Z.M.A. Judeh, C.B. Ching, S. Kawi, Catal. Lett. 85 (2003) 183.
[30] Y.C. Xiao, T.S. Chung, M.L. Chng, Langmuir 20 (2004) 8230.
[31] E.J. Acosta, C.S. Carr, E.E. Simanek, D.F. Shantz, Adv. Mater. 16 (2004) 985.
[32] V. Dufaud, M.E. Davis, J. Am. Chem. Soc. 125 (2003) 9403.
[33] A.H. Wolfgang, B. Cornils, Angew. Chem. Int. Ed. Engl. 36 (1997) 1048.
[34] L. Ropartz, R.E. Morris, D.F. Foster, D.J.C. Hamilton, Chem. Commun. (2001) 361.
[35] K. Robert, A.W. Kleij, R.J.M.K. Gebbink, G. van Koten, Top. Curr. Chem. 217 (2001) 163.
[36] D. Evans, J.A. Osborn, G. Wilkinson, J. Chem. Soc. A 12 (1968) 3133.
[37] D. Evans, G. Yagupsky, G. Wilkinson, J. Chem. Soc. A 12 (1968) 2660.
[38] M.C. Richard, B.I. Lemon III, L. Sun, L.K. Yeung, M. Zhao, Top. Curr. Chem. 212 (2001) 81.